

1
2
3
4
5
6
7
8
9
10
11
12
13
14
15
16
17
18
19
20
21
22
23
24
25
26
27
28
29
30
31
32
33
34

Technical Note:

**Spectral slopes in deep, weakly-stratified ocean
and coupling between sub-mesoscale motions
and small-scale mechanisms**
~~A note on small-
scale potential feedback mechanisms of large-
scale ocean circulations~~

by **Hans van Haren**

Royal Netherlands Institute for Sea Research (NIOZ), P.O. Box 59, 1790 AB Den Burg,
the Netherlands.
e-mail: hans.van.haren@nioz.nl

35 **Short summary.** Large ocean circulations include small-scale physical processes like transport
36 by sub-mesoscale eddies and turbulence by internal wave breaking. Knowledge is lacking on
37 precise interaction between different processes. In deep weakly stratified waters, continuous
38 spectral slopes are observed that extend from sub-mesoscales across the internal wave band to
39 turbulence range. Such cross-spectral correspondence is suggested a potential feedback
40 mechanism stabilizing large-scale ocean circulations.~~The extent of mankind's influence on~~
41 ~~Earth's climate warrants ocean studies. A supposed major heat transporter is the Atlantic~~
42 ~~Meridional Overturning Circulation (AMOC). As AMOC is a complex nonlinear dynamical~~
43 ~~system, mathematical models may predict its potential collapse using single parameters like~~
44 ~~surface temperature. However, physical processes such as (sub-)mesoscale eddy transport and~~
45 ~~turbulent mixing by internal wave breaking will alter the estimators, so that the AMOC may~~
46 ~~not collapse.~~

47

48 **Abstract.** ~~The extent of anthropogenic influence on the Earth's climate warrants studies of~~
49 ~~the ocean as a major player. Large, basin-wide ocean circulations are important for~~
50 ~~transporting properties like heat, carbon and nutrients. A supposed major conduit is the~~
51 ~~Atlantic Meridional Overturning Circulation (AMOC). As the AMOC is a Large, basin-wide~~
52 ~~ocean circulations are complex nonlinear dynamical systems, it is challenging to predict its~~
53 ~~potential to collapse and/or reversal of direction from a statistical viewpoint using a single~~
54 ~~parameter like sea surface temperature or freshwater influx in numerical models. However, as~~
55 ~~is argued in this note supported by spectra from ocean observations, They include small-scale~~
56 ~~physical processes such as, for example, transport by sub-mesoscale eddies and turbulence-~~
57 ~~generating breaking of internal waves that are not incorporated in these models will alter such~~
58 ~~parameters, and thereby statistical analyses. This may lead to feedback mechanisms on~~
59 ~~property gradients such as density stratification so that large scale ocean circulations like the~~
60 ~~AMOC may not collapse. To date however, knowledge is lacking on precise interaction~~
61 ~~between different processes. In this note, a potential contributor to interaction is investigated~~
62 ~~using spectra from deep-sea moored observations. In weakly stratified waters, continuous~~

63 spectral slopes are observed that extend from sub-mesoscales across the internal wave band to
64 turbulence range. In the latter, the governing slope can be distinctly different from the inertial
65 subrange of shear turbulence and is described as the buoyancy subrange of convection
66 turbulence. At sub-inertial frequencies, the slope's extension either describes quasi-
67 gyroscopic waves or sub-mesoscale eddies. Such cross-spectral correspondence is suggested a
68 potential feedback mechanism stabilizing large-scale ocean circulations.

69

70 **1 Introduction**

71 The extent of anthropogenic influence on the Earth's climate warrants studies of the
72 ocean as a major player. Large, basin-wide ocean circulations are important for transporting
73 properties like heat, carbon and nutrients. Schematically, the Atlantic(-Ocean) Meridional
74 Overturning Circulation (AMOC) is depicted to transport heat from the equator to the poles
75 near the surface and carbon in the abyssal return (e.g., Aldama-Campino et al., 2023). It
76 includes physical processes like 'deep dense-water formation' in the polar region. Recent
77 mathematical and numerical modelling such as based on varying single parameters like sea-
78 surface temperature (e.g., Ditlevsen and Ditlevsen, 2023) and freshwater influx (e.g., van
79 Westen et al., 2024) suggest a potential future collapse of the AMOC. It is argued that this
80 may have consequences for Northwest-European climate.

81 Whilst the modelling might be robust mathematically, it lacks physical processes of
82 the drivers of the AMOC and observational evidence thereof. This will have consequences for
83 the feedback mechanisms at work in the nonlinear dynamical system of ocean circulation. As
84 has been reviewed for AMOC numerical models (Gent, 2018), important ~~feed-back~~feedback
85 mechanisms are vertical (~~turbulent~~) mixing, (~~sub~~)mesosub-mesoscale gyre '(eddy') transport,
86 and the coupling with the atmosphere. Here we elaborate on the importance of turbulence
87 induced by internal wave breaking, possibly coupling with sub-mesoscale eddies (e.g.,
88 Chunchuzov et al., 2021), and stability variations in vertical density stratification for such
89 ~~feed-back~~feedback, by reviewing insights from recent modeling and deep-sea observations. In
90 particular as an example for complexity of dynamical system interactions, the core of ocean

91 motions is spectrally investigated focusing on most energetic mesoscale, internal wave, and
92 turbulence scales. [for deep weakly stratified waters.-](#)

93 In contrast with the atmosphere, the ocean is not an ~~in~~effective heat engine (Wunsch
94 and Ferrari, 2004) despite its heat transportation. As a result, the AMOC is not predominantly
95 buoyancy-driven via push by deep dense-water formation near the poles (Marshall and Schott,
96 1999; Marotzke and Scott, 1999), which notably occurs in sporadic pulses rather than
97 continuously. Instead, the AMOC is mainly wind-[steered \(e.g., Liu et al., 2024\)](#) and tide-
98 driven, with turbulent mixing by internal wave breaking, and possibly associated upwelling
99 close to boundaries (Ferrari et al., 2016; [McDougall and Ferrari, 2017](#)), being considered an
100 important physics process of pull that dominates over push by a heat engine. Winds, near the
101 ocean surface, and tides, via interaction with seafloor topography deeper down, contribute
102 about equally to generate internal waves that are found everywhere in the ocean interior. Such
103 waves break predominantly at ubiquitous underwater seamounts and continental slopes.

104 Without turbulent mixing, the AMOC would be confined to a 100-m thick near-
105 surface layer and the deep-ocean would be a stagnant pool of cold water (Munk and Wunsch,
106 1998). This is not the case however, and the solar heat is mixed from the surface downward
107 so that the ocean is stably stratified in density all the way into its deepest trenches, as has been
108 shown in hydrographic deep-ocean observations (Taira et al., 2005; van Haren et al., 2021a).
109 Although turbulent mixing by internal wave breaking in the ocean-interior is insufficient by at
110 least a factor of two to maintain the vertical density stratification (e.g., Gregg, 1989, Polzin et
111 al., 1997), such breaking along ocean boundaries has been suggested to be more than
112 sufficient (Munk, 1966; Polzin et al., 1997). Especially large internal wave breaking is
113 expected to occur above steeply sloping topography (Eriksen, 1982; Thorpe, 1987; Sarkar and
114 Scotti, 2017). ~~BB~~Because there are more and larger seamounts than mountains on land, equally
115 abundant sloping seafloors lead to abundant turbulent mixing, as has been charted from recent
116 observations and modelling results summarized below.

117 [As recent observations \(van Haren and Dijkstra, 2021; van Haren et al., 2024\)](#)
118 [demonstrate that breaking waves can lead to considerable buoyancy driven convection](#)

119 turbulence, this note attempts further understanding of a little studied deep-sea complex
120 process and its potential interaction with sub-mesoscale motions. The sub-inertial range of
121 sub-mesoscale motions has rarely been a subject of oceanographic spectral observations.
122 Knowledge about such small-scale processes and their interactions may be vital for
123 understanding potential feedback mechanisms affecting the stability of large-scale ocean
124 circulations.

126 **2 Recent internal wave breaking results**

127 Detailed observations and numerical modeling have revealed the extent of internal
128 tide breaking processes above ocean topography (van Haren and Gostiaux, 2012; Winters,
129 2015; Wynne-Cattanach et al., 2024). Using high-resolution observations (e.g., van Haren and
130 Gostiaux, 2012), internal tide breaking above steep deep-sea slopes is observed to generate
131 spring-neap-average turbulent vertical diffusivity value of about $3 \times 10^{-3} \text{ m}^2 \text{ s}^{-1}$. This value is
132 twice the value theoretically required to yield upwelling in a thin layer above sloping
133 topography (McDougall and Ferrari, 2017). Such qQuantification of ~~the~~ turbulent mixing
134 shows that it occurs with typical tidal-period-average values that are more than 100 times
135 larger over ~~(just)~~ super-critical slopes than open-ocean values. A super-critical seafloor slope
136 is steeper than the slope of internal wave characteristics. While ocean-wide tides energetically
137 dominate internal waves, not all seafloor slopes are super-critical for these waves. In contrast,
138 nearly all seafloor slopes are super-critical for ~~(at least one component of)~~ second~~ar~~y
139 energetic near-inertial waves, which are generated via geostrophic adjustment following the
140 passage or collapse of a disturbance such as fronts or atmospheric storms on the rotating
141 Earth. Under common stratification, near-inertial waves are at the lowest frequency of freely
142 propagating internal waves. The highest frequency propagating internal waves, near the
143 buoyancy frequency, experience ~~near~~ly vertical walls as super-critical seafloor slopes.

144 Within a tidal, or near-inertial, period, turbulence peaks in bursts of shorter duration
145 than half an hour when highly nonlinear internal waves propagate as internal bores up a
146 super-critical slope, once or twice a tidal cycle. The breaking of bores leads primarily to

147 convection~~ve~~, buoyancy-driven turbulence, rather than frictional shear-turbulence over the
148 sloping seafloor and occur at a wide variety of deep-sea and deep-ocean locations (e.g., van
149 Haren et al., 2013; van Haren et al., 2024). Between bores, the turbulent mixing varies by an
150 order of magnitude in intensity, with effects extending about 100 m vertically and several
151 kilometers horizontally from the seafloor. Although intermittently occurring at a given
152 position of the sloping seafloor and about 10% varying in arrival time, the turbulence is
153 generated internally by the tide, for about 60% (Wunsch and Ferrari, 2004), and by winds, for
154 about 40%, in a stratified ocean-environment. The turbulent bores also resuspend sediment
155 and thereby replenish nutrients away from the seafloor (Hosegood et al., 2004), important for
156 deep-sea life. Enhanced turbulent mixing above ~~(sloping)~~ boundaries has a demonstrated
157 effect on the outcome of general ocean circulation models (e.g., Scott and Marotzke, 2002),
158 with predicted subtle effects on upwelling near the seafloor (Ferrari et al., 2016).

159 The complexity of turbulence generation, mixing and restratification, are still subjects
160 of deep-ocean research. While shear-induced turbulence has been relatively well studied in
161 the stratified ocean, deviations such as convection-turbulence are little observed, with recent
162 exceptions (van Haren and Dijkstra, 2021; van Haren et al., 2024). Convection turbulence is
163 dominant in the atmosphere especially during daytime, and has also been observed in the
164 near-surface ocean during nighttime (e.g., Brainerd and Gregg, 1995), but it has never been
165 uantitatively directly observed in deep dense-water formation zones (Thorpe, 2005) and
166 above geothermal vents. question is whether the intensity of internal wave induced deep-
167 ocean turbulence is affected by variations in sea surface temperature or salinity, with what
168 consequences for the AMOC. In considering these it should be noted that various properties
169 determine different equilibria. For example, d

170 Deep dense-water formation does not only occur in polar seas, but occasionally also
171 in the at least 10°C warmer Mediterranean (Gascard, 1978), with an important contribution of
172 atmospheric exchange due to orographic generated winds affecting the preconditioning by
173 cooling and drying of near-surface waters. Similarly, internal waves occur in oceans and in
174 the Mediterranean under stratification conditions that vary over at least one order of

175 magnitude in time and space, but tides are relatively weak in the Mediterranean, and yet
176 'sufficient' turbulent diapycnal mixing, sufficient for maintenance of deep-sea stratification
177 and thereby driving overturning circulation, is generated via ~~the~~ breaking above topography
178 of near-inertial motions mainly (van Haren et al., 2013). Further complications are expected
179 from interactions of internal waves with ~~(sub-)meso~~sub-mesoscale eddies and potential
180 consequences of varying intensity thereof, e.g., on seasonal scales.

181

182 **3 Mediterranean observations as an example proxy for ocean conditions**

183 In many physical oceanographic aspects of heat and salt budgets, large-scale water-
184 flow circulation, strong boundary flow, eddies at sub-mesoscales, near-inertial motions
185 including gyrosopic waves and internal wave turbulence, the Mediterranean Sea can be
186 considered a sample for the state of the much larger oceans (e.g., Gascard, 1973; Crepon et
187 al., 1982; Garrett, 1994; Millot, 1999; van Haren and Millot, 2004; Testor and Gascard,
188 2006). Like in oceans, the Mediterranean seafloor reaches great depths and can be rugged
189 with steep slopes in places, including continental slopes incised by deep canyons.

190 In the Northwest Mediterranean, vertical density stratification varies markedly with
191 seasons and years, having relatively large near-surface values in summer and relatively low
192 values in winter. The proximity of extensive mountain ranges on land generates highly
193 variable winds that can cool and dry surface waters. In winter in weaker stratified waters, this
194 may lead to unstable conditions of buoyancy driven convection in an exchange of dense-water
195 sinking down, and less dense-waters up. Like in the polar regions, such exchange can be
196 observed daily in the upper 10 m from the sea-surface, regularly down to a few 100 m from
197 the surface, and seldom, once every 5-8 years (e.g., Rhein, 1995; Mertens and Schott, 1998),
198 down to the abyssal seafloor at about 2500 m. In contrast, horizontal density gradients
199 associate with forcing of a dynamically unstable boundary current and eddies at multiple 1-
200 100 km ~~(sub-)meso~~sub-mesoscales (e.g., Crepon et al., 1982; Testor and Gascard, 2006).
201 These eddy motions may push relatively warm waters down, thereby increasing the weak
202 stratification in the deep-sea.

203 In summer, atmospheric disturbances are less intense, near-surface stratification is
204 large due to solar heating, and eddy activity associated with some continental boundary flows
205 is weaker (Albérola et al., 1995). This opens the possibility for detection of near-inertial wave
206 dominance in kinetic energy. In relatively strong stratification, mainly gravity-driven parts of
207 near-inertial waves generate largest vertical current differences ‘shear’ that destabilize
208 stratification due to their relatively short vertical length-scale, not only in the Mediterranean
209 but also as observed in the Atlantic Ocean (van Haren, 2007). This destabilization may lead to
210 small-10-m vertical scale layering of near-homogeneous waters throughout seas and oceans.
211 On larger-100-m vertical scales near-homogeneous waters occur in deep waters of the
212 Mediterranean as well as of North-Atlantic basins like the Bay of Biscay and Canary Basin.
213 In near-homogeneous water-layers with weak stratification, gyroscopic, Earth-rotation-driven,
214 parts of near-inertial waves dominate and result in 0.1-1 km diameter smaller than ~~sub~~-sub-
215 mesoscale tubes of slantwise rather than vertical convection (Emanuel, 1994; Marshall and
216 Schott, 1999; van Haren and Millot, 2004). Hence, one may expect frequency spectra of non-
217 tidal dominated data from instruments moored in the Mediterranean reveal convection and
218 thus deep transport under winter and summer conditions.

219 It is noted that ocean-spectra may show peaks such as at narrowband tidal and at,
220 broader band, inertial frequencies, but they lack gaps. This lack of spectral gaps potentially
221 couples motions at sub-inertial with inertial-buoyancy internal wave with super-buoyancy
222 turbulence frequency ranges. However, it is unclear how such a coupling may work as some
223 motions represent two-dimensional ~~(2D)~~ eddies, some linear waves, some non-linear waves,
224 some anisotropic stratified turbulence, and some isotropic 3D turbulence. This is investigated
225 by ~~re~~(newed) spectral analysis below, using, in analogy, slopes typical for investigating
226 energy cascades in turbulence research.

227

228 **4 Uncommon slopes in revisited spectra**

229 Kinetic energy (KE) spectra from historic moored current meter observations down to
230 mid-depth $z = -1100$ m in the Ligurian Sea under upper-sea strongly stratified ‘summer’ and

231 weakly stratified ‘winter’ conditions surely lack gaps (Fig. 1). ~~Year-round at $z = -1100$ m, the~~
232 ~~buoyancy frequency N , reflecting the square-root of vertical density stratification, is small N~~
233 ~~$\sim O(f)$, f denoting the inertial frequency involving Earth rotation. This narrows the local~~
234 ~~internal wave band, while, especially in winter, sub-mesoscale activity is large in the area,~~
235 ~~and, occasionally, the few moored current meter temperature records showed inversions (van~~
236 ~~Haren and Millot, 2003).~~ Although these hourly sampled data barely resolve the turbulence
237 ranges at frequencies ~~$\omega > N$ higher than the buoyancy frequency,~~ the internal wave continuum
238 was suggested to scale ~~with frequency ω -like ω^p ,~~ with, on a log-log plot, ‘spectral slope’ $p = -$
239 ~~2.2 ± 0.4 (van Haren and Millot, 2003),~~ independent of location and season albeit with
240 different KE (power) levels.

241 Within the uncertainty range, several possible explanations can be given for the
242 observed spectral slope. ~~Freely propagating internal gravity waves have been fitted to $p = -$~~
243 ~~2 ± 0.5 but only for $f \ll \omega \ll N$ (Garrett and Munk, 1972), where f denotes the inertial~~
244 ~~frequency involving Earth rotation and N denotes the buoyancy frequency reflecting the~~
245 ~~square root of vertical density stratification.~~ Considering that the data in Fig. 1 are from a site
246 where locally $N = (3 \pm 2)f$, irrespective of season (van Haren and Millot, 2003), alternative
247 explanations were sought for observed spectral slopes at sub-inertial frequencies $0.2 \text{ cpd} < \omega$
248 $< f$. Cpd is short for ‘cycles per day’. An obvious candidate is ‘fine-structure contamination’
249 of step functions passing sensors, which gives a theoretical value of $p = -2$ (Phillips, 1971;
250 Reid, 1971). For their winter data, van Haren and Millot (2003) attributed such a slope to
251 evidence intense mesoscale activity, because of the continuation of slope up to $\omega = 5 \text{ cpd}$
252 before rolling off ~~near the Nyquist frequency to white noise (slope 0).~~ However, they did not
253 elaborate. Below, the data in Fig. 1 are re-analyzed from the perspective of convection-
254 turbulence.

255 Theoretical considerations of non-zero-mean flow convection-turbulence suggest a
256 spectral scaling in the buoyancy subrange having $p = -11/5 = -2.2$ for KE, and $p = -7/5$ for a(n
257 active) scalar quantity. This ‘BO’-scaling follows atmospheric and theoretical works by

258 Bolgiano (1959) and Obukhov (1959). The scaling was set-up for a stably stratified
259 ~~(atmospheric)~~ environment for the anisotropic part in which turbulent kinetic energy is
260 partially transferred to potential energy leading to turbulent convection. Later works extended
261 BO-scaling to purely buoyancy-driven turbulence, e.g., for Rayleigh-Bénard convection
262 (Lohse and Xia, 2010) and Rayleigh-Taylor instabilities (Poujade, 2006; Celani et al., 2006).

263 Laboratory experiments on such gravitationally driven convection are inconclusive on
264 BO-scaling. On the one hand, ~~t~~This scaling is confirmed for both KE and temperature in
265 experiments by Ashkenazi and Steinberg (1999), while on the other hand it is only confirmed
266 for scalars by Pawar and Arakeri (2016) who found a slope of $p = -5/3$ for KE. The $p = -5/3$ -
267 slope suggests dominance of shear-induced turbulence of the inertial subrange for equilibrium
268 ~~(isotropic)~~ turbulence cascade in the ‘KO’-scaling (Kolmogorov, 1941; Obukhov, 1949) but
269 should also be found in spectra of scalars that are passive in this range. While Liot et al.
270 (2016) show KO-scaling in their model that may have to do with their Lagrangian data as
271 proper transfer brings the data closer to BO-scaling, Poujade (2006) and Cenari et al. (2006)
272 show clear BO-scaling in their models. This suggests particular conditions do affect the
273 dominance of shear- or convection-turbulence. It is noted that BO-scaling is also simply
274 considered as a significant deviation from KO-scaling, which is more commonly observed in
275 stratified shear flows.

276 Obviously, scalars cannot be passive and active at the same time and in the same
277 space. This discrepancy between ~~(types of)~~ scaling between scalars and KE may be because
278 the laboratory experiments of Pawar and Arakeri (2016) were in zero mean flow. Also, under
279 sufficiently stable conditions without shear, no inertial subrange is expected (Bolgiano, 1959).
280 However, the spectral extent of BO-scaling is largely unknown albeit it is more generally
281 found adjacent to higher-frequency inertial subrange. While KO-scaling is based on a forward
282 cascade of energy, the direction of energy cascade is inconclusive for BO-scaling and may be
283 partially forward and partially backward, at least as reasoned for pure buoyancy-driven
284 convection-turbulence (Lohse and Xia, 2010). Probably, directions of cascade change with

285 locality in the flow, and perhaps depend on scale, which would also imply that KO- and BO-
 286 scaling cannot be found at the same site.

287 Revisiting data from non-zero mean flow and ~~(weakly)~~ stratified deep-sea in Fig. 1
 288 demonstrates the possibility of fit of $p = -11/5$ outside near-inertial harmonic peaks. In winter,
 289 such a fit is observed consistently through the entire range of $0.2 < \omega < 5$ cpd. In traditional
 290 terms, this frequency range covers the transition from mesoscale $\omega < f$, via internal wave $f <$
 291 $\omega < N$, to turbulence $\omega > N$ motions. In summer, the $p = -11/5$ -slope is found at two different
 292 KE levels for bands $0.2 < \omega < \omega_{\min}$ and $2\Omega < \omega < 5$ cpd at sub- and super-IGW frequencies,
 293 respectively. Here, $\omega_{\min} \leq f$ denotes the minimum frequency bound for inertio-gravity waves
 294 IGW (LeBlond and Mysak, 1978), and Ω the Earth rotational frequency. Maximum IGW
 295 frequency is denoted by $\omega_{\max} \geq 2\Omega, N$. The ω_{\min} and ω_{\max} are functions of N , latitude ϕ and
 296 direction of wave propagation (LeBlond and Mysak, 1978; Gerkema et al., 2008).

297
$$\omega_{\max}, \omega_{\min} = (A \pm (A^2 - B^2)^{1/2})^{1/2} / \sqrt{2} \tag{1}$$

 298 in which $A = N^2 + f^2 + f_s^2$, $B = 2fN$, and $f_s = f_b \sin \alpha$, α the angle to ϕ . For $f_s = 0$ or $N \gg 2\Omega$,
 299 the traditional bounds [f, N] are retrieved from (1). The plotted IGW-bounds [$\omega_{\min}, \omega_{\max}$] are
 300 for weakly stratified, near-homogeneous layers in which $N = f$. This weak stratification would
 301 lead to an impossible wave solution under the traditional approximation, but (1) allows wave
 302 propagation, albeit horizontally for one component (e.g., Gerkema et al., 2008).

303 The bridge between the KE-levels at sub- and super-IGW is formed by the finitely
 304 broad near-inertial peak. The base of this peak is proposed to slope like $p = -1$ reaching super-
 305 IGW BO-scaling at about $\omega \approx 4$ cpd $\approx N$. Such $p = -1$ -slope has been observed for the KE-
 306 spectral continuum between [f, N] from the deep Bay of Biscay, Northeast Atlantic Ocean
 307 (van Haren et al., 2002). Theoretically, this slope represents spectral scaling of intermittency
 308 of a weakly chaotic nonlinear system (Schuster, 1984), i.e., 3D dynamical systems that evolve
 309 into self-organized critical structures of states which are minimally stable (Bak et al., 1987).
 310 Such a spectral bridge, or hump, is expected for turbulence in unstable stratification, as has
 311 been illustrated using atmospheric observations (Lin, 1969). It is attributed to the flow filled

Formatted: English (United States)
 Formatted: Superscript
 Formatted: English (United States)
 Formatted: Indent: First line: 0"

312 absorbing energy from the scalar temperature field as potential energy is transferred to kinetic
313 energy. It is not clear to what extent near-inertial internal waves contribute in a similar way to
314 spectral redistribution of energy in our oceanographic data. As the observations from the
315 central Ligurian Sea show similar results, the hump is unlikely associated with seafloor slopes
316 matching the slope of near-inertial internal wave rays.

317 These spectral observations suggest a dominance of convection cascade from sub-
318 meso- via IGW- to, probably because unresolved, turbulence-scales under high-energetic
319 winter-conditions as they show a continuous slope across their frequency ranges. Such a
320 cascade is also suggested under quieter summer conditions when, however, it is masked by
321 IGW that lead a cascade at $\omega > \omega_{\min}$. Especially the sub-inertial range of apparent BO-scaling
322 seems out of the turbulence range, unless waters are near-homogeneous $N \rightarrow 0$ so that $\omega_{\min} \rightarrow$
323 0, from (1). This would extend not only IGW, notably gyroscopic waves, but also turbulence,
324 probably in the form of slantwise convection, to the ~~(sub-)meso~~sub-mesoscale range.

325 For the mesoscale range, the observations in Fig. 1 are supported by numerical
326 modeling results that have suggested eddy-KE has a broad range of spectral slopes between -3
327 $< p < -5/3$ (Storer et al., 2022), and by satellite altimetry observations that indicated, after
328 noise-correction and transfer to KE, a best-fit of $p = -2.28$ (Xu and Fu, 2012). No mention
329 was made of BO-scaling, but the correspondence seems evident.

330 As the KE in Fig. 1 is at least one order of magnitude larger in winter than in
331 summer, a near-inertial peak, if it existsent, will be part of the spectral continuum during the
332 former. The winter observations suggest a continuous spread of sub-mesoscale energy across
333 the IGW band including inertial motions and into the turbulence range. In winter, near-surface
334 stratification is considerably weaker than in summer, so that local atmospheric-generated
335 near-inertial motions will be smaller. It is noted that the signals near the Nyquist frequency
336 not only contain instrumental white noise, but also unresolved turbulence motions, which are
337 also larger in winter than in summer.

338 Inspired by Western Mediterranean observations, Saint-Guilly (1972) proposed from
339 theoretical work that winter-time inertial KE is spread over a broad featureless band, like
340 quasi-gyroscopic waves that may be present between IGW-bounds $(\frac{1}{2}f_{\min} - \omega_{\max})$ for $N \sim f$
341 (LeBlond and Mysak, 1978; Gerkema et al., 2008). However, observations from the year-
342 round upper-layer-stratified central Western Mediterranean demonstrate that, also in deep
343 homogeneous $N = 0$ waters, a near-inertial peak can be observed in KE-spectra (van Haren
344 and Millot, 2004). This may be attributed to a year-round source of atmospheric-generated
345 inertial waves that are the only internal waves that can propagate without attenuareflection
346 from well-stratified to near-homogeneous layers and vice versaback (van Haren, 2023b).

347 Based on limited spectral observations, Gascard (1973) suggested the generation of
348 12-h stability waves, (close to the buoyancy frequency of very weak stratification,) which that
349 may briefly force dense-water formation, thereby implicitly suggesting a link between
350 internal waves and (sub-)mesosub-mesoscale eddies. As such eddies have estimated relative
351 vorticity of $|\zeta| = f/2$ in the Western Mediterranean (Testor and Gascard, 2006), this addition to
352 the planetary vorticity (f) automatically widens the ‘effective’ near-inertial band $0.5f < f_{\text{eff}} <$
353 $1.5f$, of which the bounds are close to IGW-bounds for $N = 0.8f$. One of the properties can be
354 a modification of near-inertial frequency (Perkins, 1976), and trapping with downward
355 propagation of near-inertial waves in anticyclonic eddies (Kunze, 1985; Voet et al., 2024).
356 Such frequency modification may add to local physics of inertial wave caustics due to
357 latitudinal variation (LeBlond and Mysak, 1978), which however can only lead up to 15%
358 change in f in the Mediterranean. Although found to be limited to the rather flat KE-spectral
359 dip in the immediate half-order-of-magnitude sub-inertial frequency band, standing vortical
360 modes, i.e. (low-frequency non-propagating motions,) of vertical length-scale <10 m are
361 suggested to be as energetic as internal waves (Polzin et al., 2003). Alternatively, it has been
362 suggested for North-Atlantic observations that vortical modes may interact with internal
363 waves, affecting internal-wave shear that was peaking over $O(10)$ m vertical scales at IGW-

364 frequencies in a band with limits determined by weak stratification as in $N = f$ (van Haren,
365 2007).

366 For hypothetical $\omega_{\min} = 0.2$ cpd, at which the observed spectral slope changes away
367 from $p = -11/5$ (Fig. 1), one would require $N = 0.21f$, which is almost unmeasurable and ~~non-~~
368 existent for any prolonged period even in the deep Northwestern Mediterranean, to the
369 knowledge of the author. However, it may reflect ω_{\min} computed using $f_{\text{eff}} = 0.5f$ and $N = f_{\text{eff}}$,
370 noting that such conditions can only apply for part of the record. If so, it would reflect a direct
371 coupling between sub-mesoscale and IGW-motions with slantwise convection (Marshall and
372 Schott, 1999; van Haren and Millot, 2004; Gerkema et al., 2008). The $p = -11/5$ is
373 significantly distinguishable from -2 over a frequency range of nearly two orders of
374 magnitude, and from $-5/3$ over a range of just over half an order of magnitude (Fig. 1). The
375 roll-off to noise (slope 0), for $\omega > 5$ cpd, may partially be seen as following a slope of $p = -5/3$
376 before 0. The roll-off around 0.1 cpd suggests an unresolved broad mesoscale peak-value
377 between 0.01 and 0.1 cpd. While these 1980's moored current meter data barely resolved the
378 turbulence part of the KE-spectrum, and thus also not the $p=-5/3$ inertial subrange slope, their
379 temperature sensors were too poor to simultaneously verify any spectral scaling for scalars.

380 About 40 years later, high-resolution and high-precision moored temperature sensor
381 'T-' data provided opportunity to verify scalar spectral scaling of turbulence energetic
382 motions in the area. These T-data evidenced occasional warming of the deep Northwest
383 Mediterranean seafloor (Fig. 2a), which, after comparison with data from higher-up appeared
384 to be coming from above, or slanted sideways, under relatively stratified conditions, and from
385 general non-vents geothermal heating from below (van Haren, 2023a). The data were
386 collected during mid-fall, when near-surface waters were well stratified and no ~~cold, cooler~~
387 dense-water production through convection was ~~observ~~formed. Locally near the seafloor, the
388 broad two-day warming around day 308 is most stratified, whilst during other periods waters
389 are only weakly stratified, including the quasi-inertial variations between days 316 and 322.
390 These weakly stratified near-inertial, or near-buoyancy as $N \approx f$, temperature variations may

391 evidence slantwise quasi-gyroscopic near-inertial waves, which can have a large vertical
392 component (LeBlond and Mysak, 1978), as opposed to more common near-horizontal near-
393 inertial waves in strongly stratified waters that are barely noticeable in temperature records.

394 The 18-day average spectrum of the 2-s sampled data poorly resolves sub-
395 mesoscales but shows, near the seafloor, a well-resolved slope of $p = -1.4 \pm 0.025$ between a
396 large range of $0.5 < \omega < 6000$ cpd, across the IGW band and well into the turbulence band
397 (Fig. 2b). No transition to a $-5/3$ -slope is observed before roll-off to noise, but this does not
398 exclude an inertial subrange at higher frequencies hidden under white noise, although shear
399 will be limited so close to the seafloor. The observed $p = -7/5$ -slope is found significantly
400 different from $p = -2$ and $-5/3$ over the indicated frequency range of four orders of magnitude
401 and over the range between $100 < \omega < 10^4$ cpd thereby representing convection turbulence.
402 Over a frequency range of half an order of magnitude the slope-error is about ± 0.1 . Albeit not
403 greatly resolved, the range between $\omega_{\max} < \omega < 10$ cpd falls-off more steeply roughly at $p =$
404 -2 and the range between $10 < \omega < 100$ cpd shows a reduced variance that may partially be
405 characterized by intermittency ($p = -1$; Schuster, 1984), but which is not yet explained. Here,
406 it is observed to bridge between $p = -2$ and super-IGW BO-scaling $p = -7/5$. This would be
407 further observation of a marginally ocean-state to the -1 -scaling in KE-spectra (present Fig. 1
408 and van Haren et al., 2002) and in the continuum of the band [f N] in open-ocean T-spectra
409 (van Haren and Gostiaux, 2009).

410 About 140 m above the seafloor, a less precise older-type T-sensor demonstrates $p = -$
411 $7/5$ between a reduced range of about $10 < \omega < 1000$ cpd, with a suggestion for $p = -5/3$
412 around 10 cpd. This indicates convection can still dominate over shear extending O(100 m)
413 above the seafloor, as has been shown in more detail for certain periods (van Haren, 2023c).

414 Whilst more extended work with longer data sets and more T-sensors is to be done,
415 the extended continuous spectral slope from these high-resolution temperature observations
416 suggests a direct coupling between sub-mesoscale motions, IGW motions, comprising
417 internal gravity and gyroscopic waves, and convection turbulence. The temperature spectra

418 also show consistency with the limited KE-spectra of Fig. 1 from roughly the same area, and
419 both indicate a dominance of non-isotropic, stratified-turbulence convection between sub-
420 mesoscales and largest turbulent overturning scales in extended BO-scaling suggesting cross-
421 spectral coupling. The discrepancy with KE-spectra in laboratory experiments of Pawar and
422 Arakeri (2016) may be due to the difference of settings. In a non-zero-mean flow turbulence
423 convection experiment near the gas-liquid critical point, BO-scaling was observed for both
424 KE and temperature (Ashkenazi and Steinberg, 1999). We recall that our deep-sea conditions
425 are non-zero-mean flow, weak tides, very high bulk Reynolds numbers $O(10^5)$ given the
426 large scales, varying non-zero vertical density stratification, and our example spectra did not
427 clearly resolve KO-scaling.

428 This 18-day T-sensor data set demonstrates dominant deviations from inertial
429 subrange over several orders of magnitude of frequency range. The mesoscale-IGW-
430 turbulence motions transport and locally mix warm waters with cooler surroundings outside a
431 period. ~~This contrasts with the process~~ of buoyancy-driven dense-water formation, which that
432 is thought to bring cooler waters downward during short periods of time, ~~but for which no~~
433 ~~evidence exists in this 18-day T-sensor data set.~~

434

435 **5 How robust is the system of ocean circulation and stratification?**

436 Any variation to the nonlinear system of ocean circulation may encounter several
437 complex feedback mechanisms, of which the effects are not yet fully understood for the
438 present-day ocean. Although stable density stratification hampers vertical exchange by
439 turbulent mixing, it does not block it. While stratification supports internal waves and their
440 destabilizing shear, turbulent mixing during particular phase of a wave may decrease or
441 destroy it locally in time and space. However, a subsequent internal wave-phase will restratify
442 the mixed patch, thereby maintaining its own support of stable stratification. Such a feedback
443 system may be at work, for example when the ocean absorbs more heat.

444 Increased sea-surface temperature may lead to increased vertical density
445 stratification, which may lead to less turbulent exchange as vertical overturning is suppressed.

446 However, it will also lead to more internal waves through the extension of their spectral band
447 to higher frequencies, with the potential to increased interaction, non-linearity, and
448 turbulence-generating wave breaking. As particular internal waves can propagate deep into
449 the ocean interior away from their source, they can cause enhanced turbulent mixing
450 elsewhere (e.g., Alford, 2003).

451 Limited observations have thus far not provided evidence for an inverse
452 correspondence between changes in turbulent mixing and changes in temperature across the
453 near-surface photic zone along a longitudinal section of the Northeast Atlantic Ocean (van
454 Haren et al., 2021b). This lack of correspondence suggests a feedback mechanism at work
455 mediating potential physical environment changes so that global warming may not affect
456 vertical turbulent fluxes of heat, and thereby also of, e.g., carbon.

457 One such feedback mechanism may be ~~(convection-)~~turbulence induced by internal
458 waves and sub-mesoscale eddies. ~~Re(newed)~~ analysis of yearlong moored current meter data
459 from the Irminger Sea, ~~(North-Atlantic Ocean,)~~ demonstrate a significant $p = -11/5$ spectral
460 slope at sub- and at super-inertial frequencies (Fig. 3). As was outlined in van Haren (2007),
461 the area showed an IGW-band (1, for $N = f_s$) with dominant sub-inertial shear at small 8-m
462 vertical scales despite the dominant internal tidal KE. The correspondence with the
463 Mediterranean data of Fig. 1 is striking, including the one order of magnitude change in KE
464 between sub- and super-IGW $p = -11/5$ -slopes with similar $p = -1$ bridge albeit uncertain
465 crossing level, and similar heights of near-inertial peak despite the tidal peak in Fig. 3.

466 While few ocean observations have been presented of BO-scaling thus far in
467 comparison with KO-scaling, perhaps also because of the lack of precision of standard
468 oceanographic instrumentation, coupling has not been established between convection and
469 stratified small-scale turbulence with mesoscale motions. Likewise, complicating factors are
470 spectral interruption by internal waves. However, internal wave trapping by mesoscale eddies
471 has been well described (e.g., Kunze, 1985; Voet et al., 2024), and thus provides an obvious
472 coupling between these motions. It is expected that such coupling may lead to strong
473 nonlinearity ~~(of the internal waves)~~ that leads to turbulent mixing produced by wave breaking.

474 Although such turbulent mixing is smaller than that induced by internal wave breaking above
475 sloping topography, such coupling may be an important factor in downward transport of near-
476 inertial energy that eventually breaks elsewhere, e.g., over topography.

477 As demonstrated using Mediterranean observations, not only convectively unstable
478 cooler and/or saltier waters potentially lead to downward motions from the surface. Also, sub-
479 mesoscale eddies and near-inertial waves can push stratified waters to the deep sea. Such a
480 downward push can be fast to transport materials from surface to 2500-m deep seafloor in a
481 day (van Haren et al., 2006), and which ~~speed~~ is of the same order of magnitude as attributed
482 to dense-water convection (Schott et al., 1996). It can also be more turbulent compared to
483 shear-induced motions in the stratified ocean-interior, whereby turbulence reaches the
484 seafloor according to few observations from the abyssal Pacific (van Haren, 2020) and alpine
485 freshwater Lake Garda (van Haren and Dijkstra, 2021). Further extended observational
486 evidence is urgently needed, preferably resolving much larger scales.

487 Although the anthropogenic influence on the Earth's climate is without doubt, the
488 impact on ocean circulation is not fully known because we lack sufficient, notably
489 observational, information of the relevant processes that thus cannot be properly modeled yet.
490 Therefore, we should be cautious in making predictions ~~such as in~~ (e.g., Ditlevsen and
491 Ditlevsen, 2023; van Westen et al., 2024) on future ocean circulation based on single
492 parameters like ocean-surface temperature or fresh-water flux that are uncertain proxies.
493 Because no observational (van Haren et al., 2021b), modeling (Little et al., 2020) or paleo-
494 proxy validation (Cisneros et al., 2019) physics evidence exists that sea-surface temperature is
495 a solid estimator of AMOC-strength variations, other properties like vertical density gradients
496 (stratification), and turbulence intensity may be considered. Small-scale physical processes
497 such as, for example, transport by sub-mesoscale eddies and turbulence-generating breaking
498 of internal waves that are not incorporated in these models will alter such parameters, and
499 thereby statistical analyses. This may lead to feedback mechanisms on property gradients
500 such as density stratification so that large-scale ocean circulations like the AMOC may not
501 collapse.

502 Variability of the ocean in space and time is a key to its dynamics, but it is unclear
503 how robust such variations can be, e.g., whether shifting sites for deep dense-water formation
504 (Gou et al., 2024) may be part of the same system. Observational evidence verifying
505 numerical simulations' outcome, not only predictions but also present-day, of ocean-state is
506 needed. Observations are also required to ~~demonstrate evidence~~ variability in relevant physics
507 processes for model-implementation. Besides eddies and coupling with atmosphere (e.g.,
508 Gent, 2018), numerical models of complex nonlinear ocean circulation should contain
509 internal-wave turbulence with appropriate space and time dependency. The importance of
510 ~~(internal wave breaking leading to)~~ boundary mixing ~~(above sloping topography)~~ in general
511 ocean circulation models has been acknowledged in various ways (Scott and Marotzke, 2002;
512 Ferrari et al., 2016).

513 As for the ocean circulation in the horizontal plane near its surface with most impact on
514 mankind, wind will remain the main driver ~~rather than the AMOC~~. As long as the Earth
515 rotation does not alter direction, wind will maintain its general course (Wunsch, 2004). The
516 atmosphere remains the key player in the global heat transport across mid-latitudes rather than
517 the ocean. Simultaneously, the importance of processes like stratification and turbulent
518 mixing ~~is~~-induced by, e.g., internal wave breaking with or without sub-mesoscale coupling
519 cannot be underestimated for life near the ocean-surface as well as in the -deep, because it
520 will come to a halt without such processes.

521
522 *Data availability.* No new data were created or analyzed in this study: replot and re-analysis
523 of data presented in van Haren and Millot (2003), van Haren (2007) and van Haren (2023a).

524
525 *Competing interests.* The author declares that he has no conflict of interest.

526
527 *Acknowledgments.* I thank L. Gerringa for commenting on a previous draft of the manuscript.

528

529 **References**

- 530 Albérola, C., Millot, C., and Font, J.: On the seasonal and mesoscale variabilities of the
531 Northern Current during the PRIMO-0 experiment in the western Mediterranean Sea.
532 *Oceanol. Acta*, 18, 163-192, 1995.
- 533 Aldama-Campino A., Fransner F., Ödalen, M., Groeskamp, S., Yool, A. Döös, K., and
534 Nycander, J.: Meridional ocean carbon transport, *Global Biogeochem. Cy.*, 34
535 e2029GB006336, 2023.
- 536 Alford, M. H.: Redistribution of energy available for ocean mixing by long-range propagation
537 of internal waves, *Nature*, 423, 159-162, 2003.
- 538 Ashkenazi, S., and Steinberg, V.: Spectra and statistics of velocity and temperature
539 fluctuations in turbulent convection, *Phys. Rev. Lett.*, 83, 4760-4763, 1999.
- 540 Bak, P., Tang, C., and Wiesenfeld, K.: Self-organized criticality: An explanation of the 1/f
541 noise, *Phys. Rev. Lett.*, 59, 381-384, 1987.
- 542 Bolgiano, R.: Turbulent spectra in a stably stratified atmosphere, *J. Geophys. Res.*, 64, 2226-
543 2229, 1959.
- 544 [Brainerd, K. E., and Gregg, M. C.: Surface mixed and mixing layer depths, *Deep-Sea Res. I*,](#)
545 [42, 1521-1543, 1995.](#)
- 546 [Celani, A., Mazzino, A., and Vozella, L.: Rayleigh-Taylor turbulence in two dimensions,](#)
547 [*Phys. Rev. Lett.*, 96, 134504, 2006.](#)
- 548 [Chunchuzov, I. P., Johannessen, O. M., and Marmorino, G.O.: A possible generation](#)
549 [mechanism for internal waves near the edge of a submesoscale eddy, *Tellus A*, 73, 1-11,](#)
550 [2021.](#)
- 551 Cisneros, M., Cacho, I., Frigola, J., Snchez-Vidal, A., Calafat, A., Pedrosa-Pàmies, R.,
552 Rumín-Caparrós, A., and Canals, M.: Deep-water formation variability in the north-
553 western Mediterranean Sea during the last 2500 yr: A proxy validation with present-day
554 data, *Glob. Planet. Chang.* 177, 56-68, 2019.

555 Crepon, M., Wald, L., and Monget, J. M.: Low-frequency waves in the Ligurian Sea during
556 December 1977, *J. Geophys. Res.*, 87, 595-600, 1982.

557 Ditlevsen, P., and Ditlevsen, S.: Warning of a forthcoming collapse of the Atlantic meridional
558 overturning circulation, *Nat. Comm.* 14, 4254, 2023.

559 Emanuel, K., *Atmospheric Convection* 580 pp., Oxford Univ. Press, New York, 1984.

560 Eriksen, C. C.: Observations of internal wave reflection off sloping bottoms, *J. Geophys.*
561 *Res.*, 87, 525-538, 1982.

562 Ferrari, R., Mashayek, A., McDougall, T. J., Nikurashin, M. and Campin, J.-M.: Turning
563 ocean mixing upside down, *J. Phys. Oceanogr.*, 46, 2229-2261, 2016.

564 Garrett, C.: The Mediterranean Sea as a climate test basin, In: Malanotte-Rizzoli, P., and
565 Robinson, A. R. eds., *Ocean Processes in Climate Dynamics: Global and Mediterranean*
566 *Examples*, Kluwer Academic Publishes, 227-237, 1994.

567 Garrett, C., and Munk, W.: Space-time scales of internal waves, *Geophys. Fluid Dyn.*, 3, 225-
568 264, 1972.

569 Gascard, J.-C.: Vertical motions in a region of deep water formation, *Deep-Sea Res.*, 20,
570 1011-1027, 1973.

571 Gascard, J.-C.: Mediterranean deep water formation, baroclinic eddies and ocean eddies,
572 *Oceanol. Acta*, 1, 315-330, 1978.

573 Gent, P. R.: A commentary on the Atlantic meridional overturning circulation stability on
574 climate models, *Ocean Mod.*, 122, 57-66, 2018.

575 Gerkema, T., Zimmerman, J. T. F., Maas, L. R. M., and van Haren, H.: Geophysical and
576 astrophysical fluid dynamics beyond the traditional approximation, *Rev. Geophys.*, 46,
577 RG2004, doi:10.1029/2006RG000220, 2008.

578 Gou, R., Wang, Y., Xiao, K., and Wu, L.: A plausible emergence of new convection sites in
579 the Arctic Ocean in a warming climate, *Environ. Res. Lett.*, 19, 031001, 2024.

580 Gregg, M. C.: Scaling turbulent dissipation in the thermocline, *J. Geophys. Res.*, 94, 9686-
581 9698, 1989.

582 Hosegood, P., Bonnin, J., and van Haren, H.: Solibore-induced sediment resuspension in the
583 Faeroe-Shetland Channel, *Geophys. Res. Lett.*, 31, L09301, doi:10.1029/2004GL019544,
584 2004.

585

586 Kolmogorov, A. N.: The local structure of turbulence in incompressible viscous fluid for very
587 large Reynolds numbers, *Dokl. Akad. Nauk SSSR*, 30, 301-305, 1941.

588 Kunze, E.: Near-inertial wave propagation in geostrophic shear, *J. Phys. Oceanogr.*, 15, 544-
589 565, 1985.

590 LeBlond, P. H., and Mysak, L. A.: *Waves in the ocean*, Elsevier, New York, 602 pp., 1978.

591 Lin, J.-T., Turbulence spectra in the buoyancy subrange of thermally stratified shear flows,
592 143 pp., PhD-thesis Colorado State University, Fort Collins, 1969.

593 [Liot, O., Seychelles, F., Zonta, F., Chibbaro, S., Coudarchet, T., Gasteuil, Y., Pinton, J.-F.,](#)
594 [Salort, J., and Chillà, F.: Simultaneous temperature and velocity Lagrangian](#)
595 [measurements in turbulent thermal convection, *J. Fluid Mech.*, 794, 655-675, 2016.](#)

596 Little, C. M., Zhao, M., and Buckley, M. W.: Do surface temperature indices reflect
597 centennial-timescale trends in Atlantic Meridional Overturning Circulation strength?
598 *Geophys. Res. Lett.*, 47, e2020GL090888, 2020.

599 [Liu, Z., Gu, S., Zou, S., Zhang, S., Yu, Y., and He, C.: Wind-steered eastern pathway of the](#)
600 [Atlantic Meridional Overturning Circulation, *Nat. Geosci.*, 17, 353-360, 2024.](#)

601 Lohse, D., and Xia, K.-Q.: Small-Scale properties of turbulent Rayleigh-Bénard convection,
602 *Annu. Rev. Fluid Mech.*, 42, 335-364, 2010.

603 Marotzke, J., and Scott, J. R.: Convective mixing and the thermohaline circulation, *J. Phys.*
604 *Oceanogr.*, 29, 2962-2970, 1999.

605 Marshall, J., and Schott, F.: Open-ocean convection: observations, theory, and models, *Rev.*
606 *Geophys.*, 37, 1-64, 1999.

607 [McDougall, T. J., and Ferrari, R.: Abyssal upwelling and downwelling driven by near-](#)
608 [boundary mixing, *J. Phys. Oceanogr.*, 47, 261-283, 2017.](#)

Formatted: Indent: Left: 0", First line: 0"

609 Mertens, C., and Schott, F.: Interannual variability of deep-water formation in the
610 Northwestern Mediterranean, *J. Phys. Oceanogr.*, 28, 1410-1424, 1998.

611 Millot, C.: Circulation in the Western Mediterranean Sea, *J. Mar. Sys.*, 20, 423-442, 1999.

612 Munk, W.: Abyssal recipes, *Deep-Sea Res.*, 13, 707-730, 1966.

613 Munk, W., and Wunsch, C.: Abyssal recipes II: Energetics of tidal and wind mixing, *Deep-*
614 *Sea Res. I*, 45, 1977-2010, 1998.

615 Obukhov, A. M.: Structure of the temperature field in a turbulent flow, *Izv. Akad. Nauk*
616 *SSSR, Ser. Geogr. Geofiz.*, 13, 58-69, 1949.

617 Obukhov, A. M.: Effect of buoyancy forces on the structure of temperature field in a turbulent
618 flow, *Dokl. Akad. Nauk SSSR*, 125, 1246-1248, 1959.

619 Pawar, S. S., and Arakeri, J. H.: Kinetic energy and scalar spectra in high Rayleigh number
620 axially homogeneous buoyancy driven turbulence, *Phys. Fluids*, 28, 065103, 2016.

621 Perkins, H.: Observed effect of an eddy on inertial oscillations, *Deep-Sea Res.*, 23, 1037-
622 1042, 1976.

623 Phillips, O. M.: On spectra measured in an undulating layered medium, *J. Phys. Oceanogr.*, 1,
624 1-6, 1971.

625 Polzin, K. L., Toole, J. M., Ledwell, J. R., and Schmitt, R. W.: Spatial variability of turbulent
626 mixing in the abyssal ocean, *Science*, 276, 93-96, 1997.

627 Polzin, K. L., Kunze, E., Toole, J. M., and Schmitt, R. W.: The partition of finescale energy
628 into internal waves and subinertial motions, *J. Phys. Oceanogr.*, 33, 234-248, 2003.

629 [Poujade, O.: Rayleigh-Taylor turbulence is nothing like Kolmogorov turbulence in the self-](#)
630 [similar regime, *Phys. Rev. Lett.*, 97, 185002, 2006.](#)

631 Reid, R. O.: A special case of Phillips' general theory of sampling statistics for a layered
632 medium, *J. Phys. Oceanogr.*, 1, 61-62, 1971.

633 Rhein, M.: Deep water formation in the western Mediterranean, *J. Geophys. Res.*, 100, 6943-
634 6959, 1995.

635 Saint-Guiluy, B.: On the response of the ocean to impulse, *Tellus* 24, 344-349, 1972.

636 Sarkar, S., and Scotti, A.: From topographic internal gravity waves to turbulence, *Ann. Rev.*
637 *Fluid Mech.*, 49, 195-220, 2017.

638 Schott, F., Visbeck, M., Send, U, Fischer, J., and Desaubies, Y.: Observations of deep
639 convection in the Gulf of Lions, Northern Mediterranean, during the winter of 1991/92, *J.*
640 *Phys. Oceanogr.*, 26, 505-524, 1996.

641 Schuster, H. G., *Deterministic Chaos: An Introduction*, Physik-Verlag, Weinheim, 220 pp.,
642 1984.

643 Scott, J. R., and Marotzke, J, 1998: The location of diapycnal mixing and the meridional
644 overturning circulation, *J. Phys. Oceanogr.*, 32, 3578-3595, 2002.

645 Storer, B. A., Buzzicotti, M., Khatri, H., Griffies, S. M., and Aluie, H.: Global energy
646 spectrum of the general oceanic circulation, *Nat. Comm.*, 13, 5314, 2022.

647 Taira, K., Yanagimoto D., and Kitagawa, S.: Deep CTD casts in the challenger deep. Mariana
648 Trench, *J. Oceanogr.*, 61, 447-454, 2005.

649 Testor, P., and Gascard, J.C.: Post-convection spreading phase in the Northwestern
650 Mediterranean Sea, *Deep-Sea Res.*, 53, 869-893, 2006.

651 Thorpe, S. A.: Transitional phenomena and the development of turbulence in stratified fluids:
652 a review, *J. Geophys. Res.*, 92, 5231-5248, 1987.

653 [Thorpe, S. A.: The turbulent ocean. Cambridge University Press, Cambridge, 439 pp, 2005.](#)

654 van Haren, H.: Inertial and tidal shear variability above Reykjanes Ridge, *Deep-Sea. Res. I.*
655 54, 856-870, 2007.

656 van Haren, H.: Slow persistent mixing in the abyss, *Ocean Dyn.*, 70, 339-352, 2020.

657 van Haren, H.: Convection and intermittency noise in water temperature near a deep
658 Mediterranean seafloor, *Phys. Fluids*, 35, 026604, 2023a.

659 van Haren, H.: Near-inertial wave propagation between stratified and homogeneous layers, *J.*
660 *Oceanogr.*, 79, 367-377, 2023b.

661 [van Haren, H.: Direct observations of general geothermal convection in deep Mediterranean](#)
662 [waters. Ocean Dyn., 73, 807-825, 2023c.](#)

663 van Haren, H., and Dijkstra, H. A.: Convection under internal waves in an alpine lake, *Env.*
664 *Fluid Mech.*, 21, 305-316, 2021.

665 van Haren, H., and Gostiaux, L.: High-resolution open-ocean temperature spectra, *J.*
666 *Geophys. Res.*, 114, C05005, doi:10.1029/2008JC004967, 2009.

667 van Haren, H., and Gostiaux, L.: Detailed internal wave mixing observed above a deep-ocean
668 slope, *J. Mar. Res.*, 70, 173-197, 2012.

669 van Haren, H. and Millot, C.: Seasonality of internal gravity waves kinetic energy spectra in
670 the Ligurian Basin, *Oceanol. Acta*, 26, 635-644, 2003.

671 van Haren, H., and Millot, C.: Rectilinear and circular inertial motions in the Western
672 Mediterranean Sea, *Deep-Sea Res. I*, 51, 1441-1455, 2004.

673 van Haren, H., Maas, L., and van Aken, H.: On the nature of internal wave spectra near a
674 continental slope, *Geophys. Res. Lett.*, 29(12), 10.1029/2001GL014341, 2002.

675 van Haren, H., Millot, C., and Taupier-Letage, I.: Fast deep sinking in Mediterranean eddies,
676 *Geophys. Res. Lett.*, 33, L04606, doi:10.1029/2005GL025367, 2006.

677 van Haren, H., Ribó, M., and Puig, P.: (Sub-)inertial wave boundary turbulence in the Gulf of
678 Valencia. *J. Geophys. Res. Oceans*, 118, 2067-2073, doi:10.1002/jgrc.20168, 2013.

679 van Haren, H., Uchida, H., and Yanagimoto, D.: Further correcting pressure effects on
680 SBE911 CTD-conductivity data from hadal depths, *J. Oceanogr.*, 77, 137-144, 2021a.

681 van Haren, H., Brussaard, C. P. D., Gerringa, L. J. A., van Manen, M. H., Middag, R., and
682 Groenewegen, R.: Diapycnal mixing near the photic zone of the NE-Atlantic, *Ocean Sci.*,
683 17, 301-318, 2021b.

684 van Haren, H., Voet, G., Alford, M. H., Fernandez-Castro, B., Naveira Garabato, A. C.,
685 Wynne-Cattanach, B. L., Mercier, H., and Messias, M.-J.: Near-slope turbulence in a
686 Rockall canyon, *Deep-Sea Res. I*, 206, 104277, 2024.

687 van Westen, R. M., Kliphuis, M., and Dijkstra, H.A.: Physics-based early warning signal
688 shows that AMOC is on tipping course, *Sci. Adv.*, 10, eadk1189, 2024.

689 Voet, G., et al.: Near-inertial energy variability in a strong mesoscale eddy field in the Iceland
690 Basin, *Oceanogr.*, 37, <https://doi.org/10.5670/oceanog.2024.302>, 2024.

691 Winters, K. B.: Tidally driven mixing and dissipation in the stratified boundary layer above
692 steep submarine topography, *Geophys. Res. Lett.*, 42, 7123-7130, 2015.

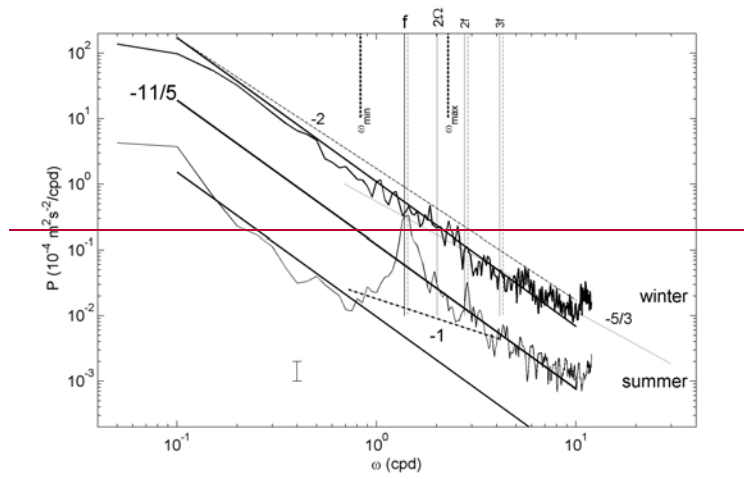
693 Wunsch, C.: Gulf Stream safe if wind blows and Earth turns, *Nature*, 428, 601, 2004.

694 Wunsch, C., and Ferrari, R.: Vertical mixing, energy and the general circulation of the oceans,
695 *Ann. Rev. Fluid Mech.*, 36, 281-314, 2004.

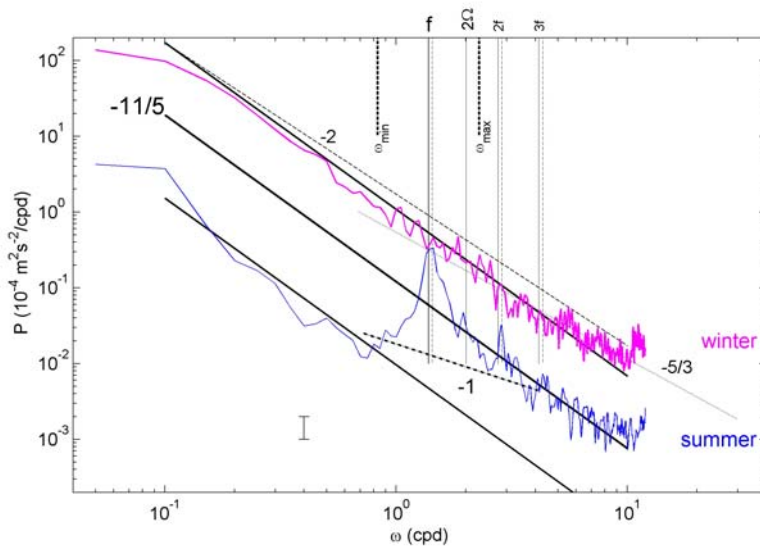
696 Wynne-Cattanach, B. L., Couto, N., Drake, H. F., Ferrari, R., Le Boyer, A., Mercier, H.,
697 Messias, M.-J., Ruan, X., Spingys, C. P., van Haren, H., Voet, G., Polzin, K., Naveira
698 Garabato, A., and Alford, M. H.: Observational evidence of diapycnal upwelling within a
699 sloping submarine canyon, *Nature*, 630, 884-890, 2024.

700 Xu, Y., and Fu, L.-L.: The effects of altimeter instrument noise on the estimation of the
701 wavenumber spectrum of sea surface height, *J. Phys. Oceanogr.*, 42, 2229-2233, 2012.
702

Formatted: Indent: Left: 0", First line: 0"



704

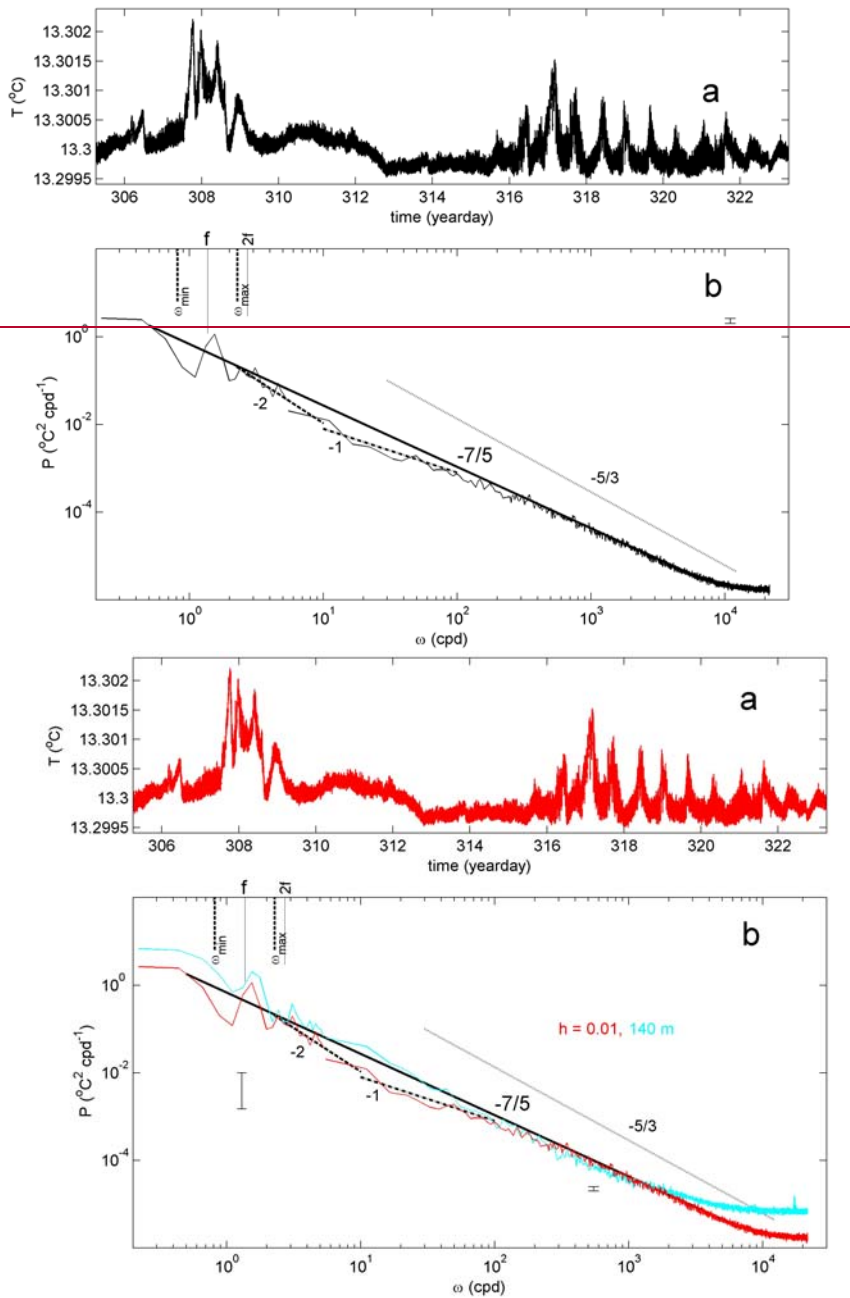


705

706 **Fig. 1.** Moderately smoothed (20 degrees of freedom, dof) kinetic energy (KE) spectra over
 707 100 days of data from 3600-s sampled Aanderaa mechanical current meter moored in
 708 1981/1982 at $z = -1100$ m well above the continental slope in the Ligurian Sea at 43°
 709 $28.32'$ N, $7^\circ 46.10'$ E, 2250 m water depth. For details on these data, see van Haren and

Formatted: Line spacing: 1.5 lines

710 Millot (2003). The two spectra are not offset deliberately from each other; 'noise' also
711 contains other signals near the Nyquist frequency. The 'summer' spectrum (blue) is an
712 average from data between days 190 and 290 (in 1981), the 'winter' (magenta) between days
713 375 and 475 (adding +365 for days in 1982). Several frequencies are indicated including
714 ~~inertial frequency~~ inertial frequency f , Earth rotational Ω and inertio-gravity wave bounds
715 [$\omega_{\min} \leq f$, $\omega_{\max} \geq N$, 2Ω] for ~~buoyancy frequency~~ buoyancy frequency $N = f$. The dashed lines
716 indicate (harmonics of) $1.04f$. Four spectral slopes ω^p are indicated by their exponent: $p = -$
717 $11/5$ (solid slope in the log-log plot) for Bolgiano-Obukhov 'BO' scaling reflecting the
718 buoyancy subrange of ~~convective turbulence~~ convection-turbulence (e.g., Pawar and Arakeri,
719 2016), $p = -5/3$ (dotted slope) for Kolmogorov-Obukhov 'KO' scaling reflecting the
720 equilibrium inertial subrange for dominant shear-induced turbulence (Kolmogorov 1941;
721 Obukhov, 1949), $p = -1$ (dash-dotted slope) for intermittency of self-organized criticality
722 (Schuster, 1984; Bak et al., 1987) and $p = -2$ (dashed slope) for internal wave scaling (Garrett
723 and Munk, 1972) or finestructure contamination (Phillips, 1971; Reid, 1971).
724



725

726

727

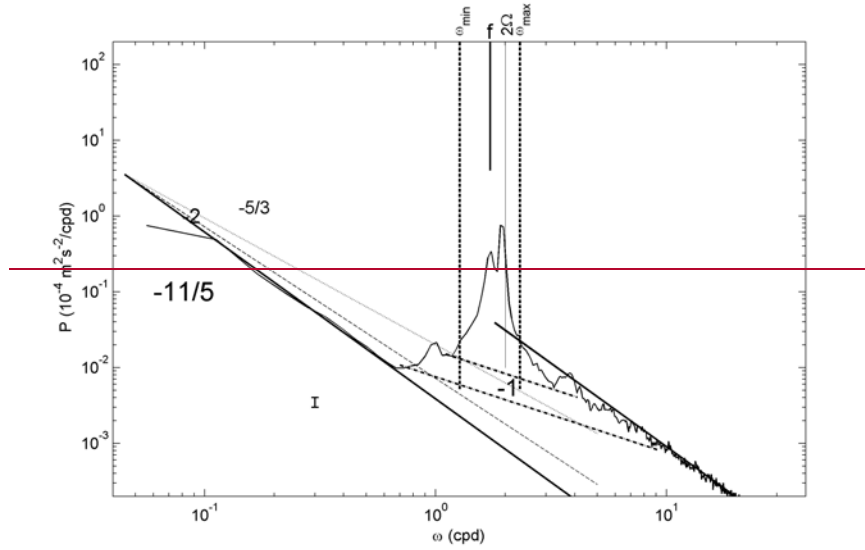
728

729

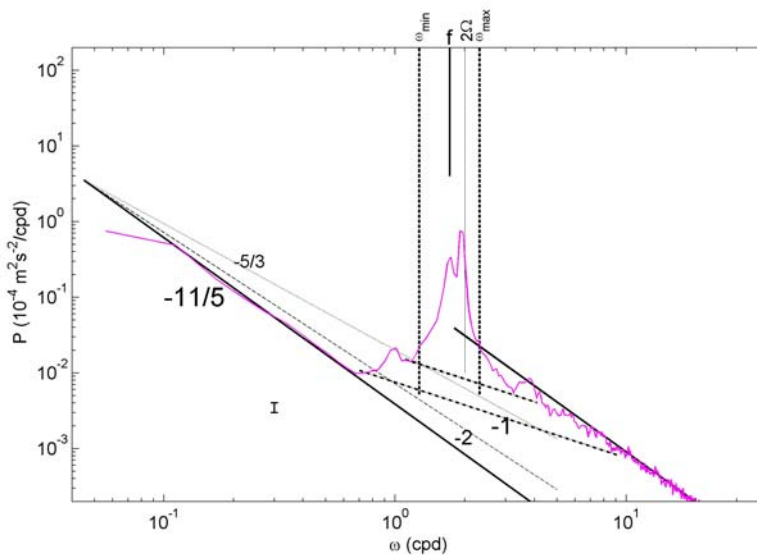
730

Fig. 2. Eighteen days of high-resolution 2-s sampled temperature $\langle T \rangle$ data from a NIOZ T-sensor fallen off a mooring-line in 2020 and lying 0.01 m above a flat seafloor about 10 km south of the foot of the continental slope at $42^\circ 49.50' N$, $6^\circ 11.78' E$, 2458 m water depth, about 100 km WSW from the site in Fig. 1. For details on these data see van Haren

731 (2023a). (a) Time series of 18 days of raw temperature data. (b) Temperature variance
732 spectrum that is stitched together using two spectra with different smoothing. Weakly
733 smoothed (10 dof; $\omega < 5$ cpd) and heavily smoothed (250 dof; $\omega > 5$ cpd) ~~temperature~~
734 ~~variance~~-spectra of data in a., with bars showing the respective 95% confidence limits.
735 For comparison, a spectrum is shown in cyan from data of a less precise T-sensor at a
736 drag-parachute line stuck at 140 m above the seafloor. Frequency and spectral slope
737 indications are as in Fig. 1, while $-7/5$ (solid slope) indicates BO-scaling of an active
738 scalar (e.g., Pawar and Arakeri, 2016), ~~and -1 (dash-dotted slope) for scaling of~~
739 ~~intermittency of a weakly chaotic nonlinear system (Schuster, 1984).~~ Note the different
740 axes-ranges compared with Fig. 1.



741



742

743

744

745

Fig. 3. Like Fig. 1 with the same axes ranges, but for strongly smoothed (50 dof) KE spectra averaged over 400 days of data from 600-s sampled Valeport mechanical current meter moored at $z = -1000$ m over the Mid-Atlantic Ridge at $58^\circ 59.67'$ N, $33^\circ 56.12'$ W,

746 2540 m water depth in 2003/2004, within the project discussed in van Haren (2007). The
747 small bar shows the 95% confidence interval.
748